ResearchGate

See discussions, stats, and author profiles for this publication at: https://www.researchgate.net/publication/231015801

Different tendencies of breakdown threshold on pulse duration in the subpicosecond regime in fused silica

Article *in* Journal of Optics A Pure and Applied Optics · March 2005

DOI: 10.1088/1464-4258/7/4/008

CITATIONS
8

READS
39

6 authors, including:

Hongbing Jiang
Peking University
73 PUBLICATIONS **765** CITATIONS
SEE PROFILE

Quan Sun
Hokkaido University
36 PUBLICATIONS **466** CITATIONS
SEE PROFILE

Zhaoxin Wu
Xi'an Jiaotong University
115 PUBLICATIONS **991** CITATIONS
SEE PROFILE

All content following this page was uploaded by Quan Sun on 01 December 2014.

The user has requested enhancement of the downloaded file.

IOPscience iopscience.iop.org

Home Search Collections Journals About Contact us My IOPscience

Different tendencies of breakdown threshold on pulse duration in the subpicosecond regime in fused silica

This article has been downloaded from IOPscience. Please scroll down to see the full text article.

2005 J. Opt. A: Pure Appl. Opt. 7 198

(http://iopscience.iop.org/1464-4258/7/4/008)

The Table of Contents and more related content is available

Download details:
IP Address: 133.87.246.56
The article was downloaded on 29/03/2010 at 02:17

Please note that terms and conditions apply.

INSTITUTE OF PHYSICS PUBLISHING JOURNAL OF OPTICS A: PURE AND APPLIED OPTICS
J. Opt. A: Pure Appl. Opt. **7** (2005) 198–203 doi:10.1088/1464-4258/7/4/008

Different tendencies of breakdown threshold on pulse duration in the subpicosecond regime in fused silica

Yi Liu, Hongbing Jiang, Quan Sun, Zhaoxin Wu, Hong Yang and Qihuang Gong

State Key Laboratory for Mesoscopic Physics and Department of Physics, Peking University, Beijing 100871, People's Republic of China

E-mail: hbjiang@pku.edu.cn and qhgong@pku.edu.cn

Received 30 October 2004, accepted for publication 9 February 2005
Published 9 March 2005
Online at stacks.iop.org/JOptA/7/198

Abstract
Measurements of the single-shot laser-induced breakdown threshold in bulk fused silica were performed at a wavelength of 800 nm for pulse durations ranging from 240 fs to 2.5 ps. Objectives with different numerical apertures (NAs) were used to focus the laser pulse into the sample. It was found that the threshold started to increase with the decrease of the pulse duration when it was less than 700 fs for effective NA = 0.126, while for effective NA = 0.255 it kept decreasing. Numerical simulations based on the nonlinear propagation model revealed that the generated plasma played an important role in the breakdown process and was responsible for the different tendencies observed in this study. Moreover, it was noticeable that the trend of the threshold on pulse duration was sensitive to the assumed threshold electron density, which implied that various definitions of breakdown might lead to different tendencies of the threshold.

Keywords: breakdown threshold, subpicosecond, fused silica

1. Introduction

Laser-induced breakdown (LIB) of transparent dielectric materials has been the subject of extensive experimental and theoretical investigations since the laser was invented 40 years ago [1–9]. Despite the long history, LIB remains an active area of research not only because it could help to understand the mechanism of ionization induced by the laser pulse, but also because the damage to the optical components resulting from LIB is often the restriction on system performance in high-power laser applications [10]. Optical breakdown in transparent materials is associated with the rapid buildup of conduction electrons to a critical density. For long pulses, conduction electrons are generated by background carrier seeded impact ionization that leads to avalanche [1]. And there exists an empirical scaling law of the breakdown threshold fluence $F_{th} \propto \tau_p^{0.5}$, where τ_p is the pulse duration [11].

Several recent experiments have studied LIB or laser-induced damage of fused silica as a function of laser pulse duration that has been extended to the femtosecond regime [2–8]. Du *et al* collected the plasma emission from the focal region to determine the breakdown threshold of a thin bulk sample, and they reported an increase of the thresholds with the decrease of the pulse duration for $\tau_p < 1$ ps. Their observations were mainly explained in terms of an impact ionization rate scaling with the square root of the laser intensity [2, 3]. In contrast to Du, Stuart *et al* studied the damage on the surface of a fused silica sample and found no evidence for the increase of damage threshold with the decrease of pulse duration, although a deviation from the $\tau_p^{0.5}$ scaling rule was observed [4, 5]. Theoretically, they proposed a linear dependence of impact ionization rate on laser intensity and found good agreement with their experimental results. Later, Varel *et al* [6], Lenzner *et al* [7], and Tien *et al* [8] confirmed the tendency of surface breakdown thresholds observed by Stuart *et al*. To interpret these inconsistent observations, the combination of Thornber's model for avalanche and Keldysh's formula for photoionization was employed [8]. The numerical results

from this model suggested different tendencies of breakdown threshold and it was found that the initial free electron densities of the samples were responsible for it, which needs further experimental validation.

Measurements on the entrance surface of the sample were preferred by the researchers due to the fact that the effect of self-focusing (SF) could be undoubtedly excluded in this way [4–8]. However, some researchers suspected that surface thresholds were possibly lowered by contamination or surface defects [9], which made it difficult to compare the experimental results of various research groups. Furthermore, up to now most of the existing models [2, 4, 8] which have been used to describe the thresholds for surface LIB or damage did not take into account any surface effects such as the escape of electrons from the surface [12].

Recently the breakdown threshold energy inside bulk transparent material as a function of focusing conditions for fixed pulse duration has been investigated. Schaffer *et al* determined the laser-wavelength and material band-gap dependence of the threshold energy [13], while Nguyen *et al* investigated the formation conditions of optical breakdown and filamentation [14]. In this paper we report the study on the thresholds of LIB inside fused silica as a function of pulse duration. In the experiments, it was found that when the focusing condition was changed the threshold energy exhibited different tendencies in the subpicosecond regime. We systematically simulated the tendencies by a nonlinear propagation model and found good agreement with our experimental results. The calculation indicated that the defocusing effect of the generated plasma played a crucial role in the breakdown process and was responsible for our observed different tendencies. In addition, it was found that the predicted threshold would exhibit diverse tendencies when different threshold electron densities were chosen as the criterion of breakdown.

2. Experimental setup

The experimental setup is almost the same as that reported in our previous work [15]. The laser pulse was first spatially filtered and then focused into the sample by objectives with numerical aperture NA = 0.4 or 0.85. The diameter of the collimated beam before entering the objective could be varied by changing the collimating lens with different focus length. In the experiments we underfilled the incident aperture of the objectives by a factor of about 3. In this way the diffraction induced by the objective was avoided and a spatial Gaussian distribution of the laser beam after the objective was achieved. In our experiments the radius ω of the beam just after the objective and the distance d between this position and the focus were measured by a knife-edge method. We defined the effective NA $= \omega/(\omega^2 + d^2)^{0.5}$. In this way the effective NAs corresponding to the two focusing conditions were calculated to be 0.126 and 0.255. According to a Gaussian beam the radius of the pulse at the focus can be estimated to be 2.0 and 0.95 μm respectively. In these cases the spherical aberration introduced by focusing into the bulk of sample was expected to be small because the practical NA was less than 0.5 [13].

In order to avoid any surface effects and to examine the influence of focus depth inside the sample, we have done the measurements under different depths. The surfaces of the fused silica were polished, and the size of the sample was $10 \times 5 \times 3$ mm^3. It was mounted on an xyz translation stage to ensure that the laser pulse irradiated each location of the sample only once. The plasma luminescence was imaged from the side by a highly sensitive cooled charge coupled device (CCD) camera (Princeton Instruments, TE/CCD-512/SB) with the aid of another objective. The spectral range of the CCD is 190–1080 nm and the quantum efficiency is above 70% in the range of 300–800 nm. In the experiments a filter to block the diffracted laser pulse at 800 nm is used in front of the CCD. Interaction of a single laser pulse with the sample was achieved with a shutter during the exposure time of the CCD camera.

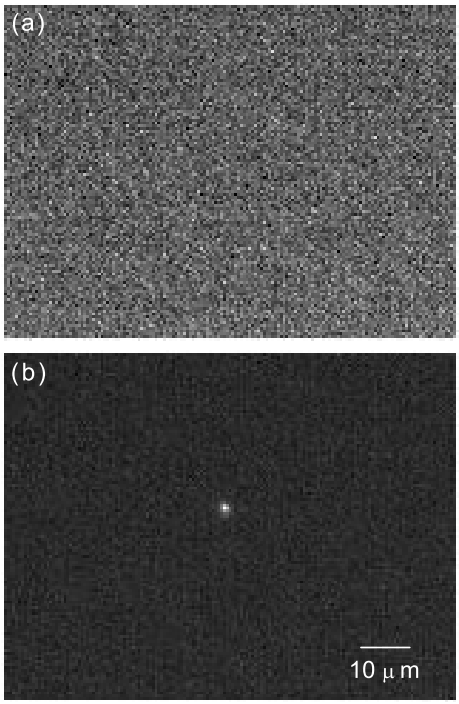

Figure 1. Images of the plasma emission in the case of NA = 0.255 for $\tau_p = 400$ fs. (a) $E_{in} = 0.17$ μJ, (b) $E_{in} = 0.18$ μJ. The incident direction of the laser pulse is from right to left.

3. Experimental results and discussion

In the experiments we changed the pulse duration by adjusting the compression grating of the laser system, and for each duration we modulated the input pulse energy (E_{in}) and obtained the image of the excited region. Typical images of the plasma emission in the case of NA = 0.255 are displayed in figure 1 for $\tau_p = 400$ fs. For $E_{in} = 0.17$ μJ, an image of pure noise is obtained while for $E_{in} = 0.18$ μJ a clear image of the plasma can be seen. Therefore the threshold in this case can be defined as 0.18 μJ with an error of 0.01 μJ. In this way the threshold corresponding to different pulse duration can be well defined.

As mentioned above, we have measured the threshold energies under different depths inside the sample, namely, 6 ± 5 μm, 170 ± 5 μm and 300 ± 5 μm. We found that for fixed pulse duration the threshold had a slight decrease when the laser pulse was focused deeper inside the sample and

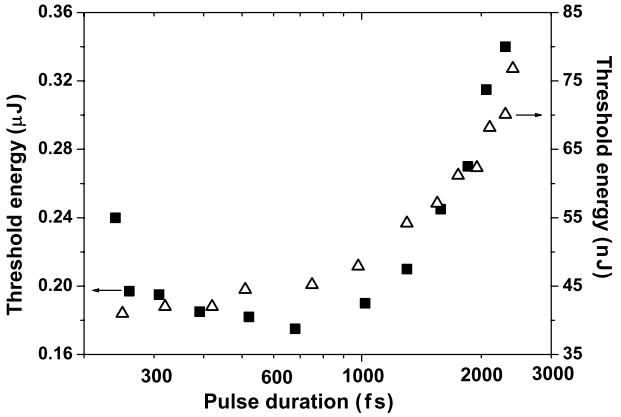

Figure 2. Experimental results of threshold energies in fused silica at a wavelength of 800 nm. Squares: effective NA = 0.126; triangles: effective NA = 0.255.

the maximum variation of the threshold for the three depths was within ten per cent. However, the respective tendency of threshold was the same for these three focus depths. Therefore we thought that in our experiments the influence of the spherical aberration on our observed tendencies of the threshold was insignificant. We performed the measurements in detail at 300 μm depth from the surface, and the results are shown in figure 2 as a function of laser pulse duration for the two focusing conditions. In the case of effective NA = 0.126, an increase of the thresholds for pulse duration shorter than 700 fs was observed. In contrast, for effective NA = 0.255 the breakdown threshold kept decreasing when the pulse duration was reduced from 2.5 ps to 240 fs. As mentioned above, some researchers attributed the various tendencies to the difference in initial electron density [8]. However, in our experiments the same samples were used all the time, therefore the initial electron density could be excluded as a reason that accounts for the different tendencies. The focusing condition dependence indicated that some effects in the course of nonlinear propagation must be responsible for the observed different tendencies.

We employed a three-dimensional model to simulate the breakdown process in the sample. A linearly polarized incident beam with cylindrical symmetry around the propagation axis is considered. The electric field is written as $E = \mathrm{Re}[\varepsilon \exp(\mathrm{i}kz - \mathrm{i}\omega_0 t)]$, where $k = n_0\omega_0/c$ and ω_0 are the wavenumber and the frequency of the carrier wave. The evolution of the complex envelope ε can be modelled with the following equation expressed in the reference frame moving at the group velocity [16]:

$$\left(\mathrm{i}2k\frac{\partial}{\partial z} + \nabla_\perp^2\right)\varepsilon = kk''\frac{\partial^2\varepsilon}{\partial^2\xi} - 2kk_0n_2|\varepsilon|^2\varepsilon - \mathrm{i}k\sigma(1 + \mathrm{i}\omega_0\tau_c)\rho\varepsilon - \mathrm{i}k\beta^{(K)}|\varepsilon|^{2K-2}\varepsilon \quad (1)$$

where ξ refers to the retarded time variable $t - z/v_g$ with group velocity v_g. The Laplacian describes the diffraction in the transverse plane and k'' is the group velocity dispersion (GVD) coefficient. The following terms in equation (1) account for the Kerr effect of the material with $n_2 = 3.54 \times 10^{-16}$ cm^2 W^{-1} [17], plasma absorption, defocusing with electron density ρ, and multiphoton absorption (MPA) with coefficient $\beta^{(K)} = K\hbar\omega_0\sigma_K\rho_{at}$. A band gap potential E_g = 9 eV of the material yields the $K = 6$ required for the ionization and the multiphoton ionization (MPI) coefficient $\sigma_K = 9.8 \times 10^{-70}$ s^{-1} cm^{12} W^{-6} [17]. The cross-section for inverse bremsstrahlung reads $\sigma = ke^2\tau_c/\omega_0 m_e\epsilon_0(1 + (\omega_0\tau_c)^2) = 1.55 \times 10^{-18}$ cm^2, where the electron collision time $\tau_c = 2.33 \times 10^{-14}$ s [17]. The critical plasma density ρ_c, and the background atom density, $\rho_{at} = 2.1 \times 10^{21}$ cm^{-3}, are in the ratio $\rho_{at}/\rho_c \approx 12$ [18]. Assuming that both avalanche and MPI contribute to the generation of the conduction electron, then ρ satisfies the following evolution equation:

$$\frac{\partial\rho}{\partial\xi} = \frac{\sigma}{n_0^2 E_g}\rho|\varepsilon|^2 + \sigma_K\rho_{at}|\varepsilon|^{2K}. \quad (2)$$

The first term on the right-hand side of equation (2) accounts for impact ionization. This avalanche rate comes from Drude model and has been widely used in solids, water and gases [17, 19, 20]. The second term describes the MPI contribution, which is not expressed by Keldysh's formula for photo ionization because the adiabaticity parameter $\gamma \gg 1$ in our experiments. As to the electron recombination process, some researchers did not take it into consideration [2, 4] while others did [18, 19]. In our simulations it was not considered. We have performed simulations for typical pulse durations with consideration of it, and just found a slight variant. In our simulations $\rho_0 = 1.0 \times 10^8$ cm^{-3} is adopted as the initial electron density [8].

The breakdown threshold can be predicted by postulating a threshold electron density associated with the occurrence of LIB and solving the coupled equations. An alternating direction implicit method (ADI) was used to solve equation (1) with initial conditions corresponding to our experiments. In all our simulations it is found that the plasma density in fused silica tends to saturate under 10^{19} cm^{-3}, although the specific quantity depends on the focusing conditions and the pulse duration, which agrees with the theoretical result of Ward [18] and our recent measurements [21]. Four threshold electron densities are assumed in the calculation for NA = 0.126, and the theoretical results are shown in figure 3(a). In the case of $\rho_{th} = 1.8 \times 10^{19}$ cm^{-3} and $\rho_{th} = 1.45 \times 10^{19}$ cm^{-3}, the predicted thresholds start to increase when the pulse duration becomes shorter than 1000 and 550 fs, respectively. However, the threshold energies remain almost constant after 500 fs for $\rho_{th} = 1.3 \times 10^{19}$ cm^{-3} while they keep decreasing for $\rho_{th} = 1.0 \times 10^{19}$ cm^{-3}. Here we would like to mention the previous work of Guo *et al* in our group, in which they studied the damage threshold and refractive index change threshold of fused silica with an objective of effective NA = 0.08 [22]. They found that after τ_p is less than 230 fs, the damage threshold begins to increase significantly while the refractivity change threshold keeps decreasing with the decrease of the pulse duration. It is natural that the electron density corresponding to damage is higher than that of the refractive index change. Therefore this observation could be deemed as an experimental proof of our above prediction, although the definition of threshold in their work differs from our definition of LIB. In figure 3(b) the calculated thresholds from two threshold electron densities in the case of NA = 0.255 are displayed. For $\rho_{th} = 1.45 \times 10^{19}$ cm^{-3}, the threshold energy decreases dramatically with the decrease of the pulse duration, while for

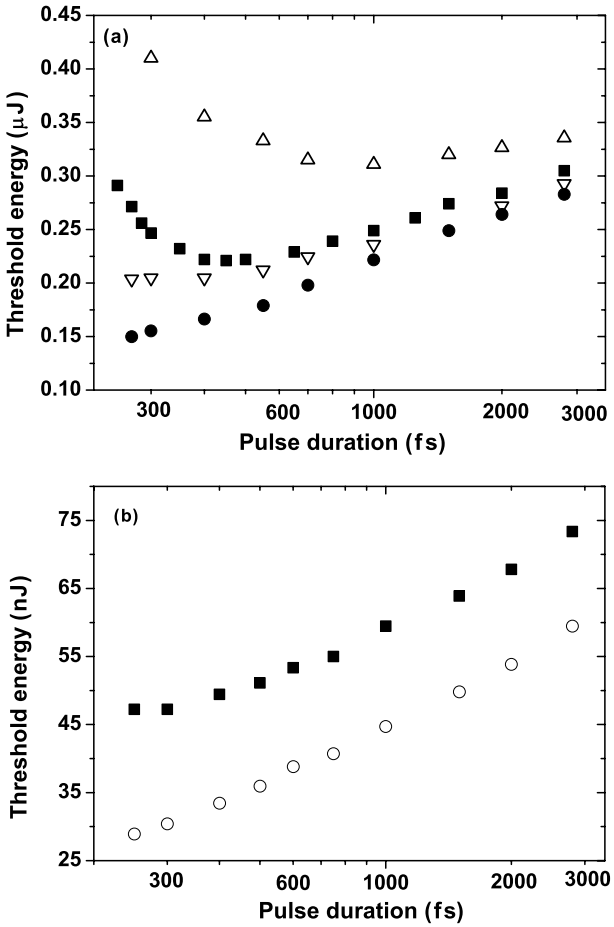

Figure 3. Breakdown threshold energies calculated from different threshold electron densities. (a) Effective NA = 0.126, circles: $\rho_{th} = 1.0 \times 10^{19}$ cm^{-3}; down triangles: $\rho_{th} = 1.3 \times 10^{19}$ cm^{-3}; squares: $\rho_{th} = 1.45 \times 10^{19}$ cm^{-3}; up triangles: $\rho_{th} = 1.8 \times 10^{19}$ cm^{-3}. (b) Effective NA = 0.255, circles: $\rho_{th} = 1.45 \times 10^{19}$ cm^{-3}; squares: $\rho_{th} = 6.11 \times 10^{19}$ cm^{-3}.

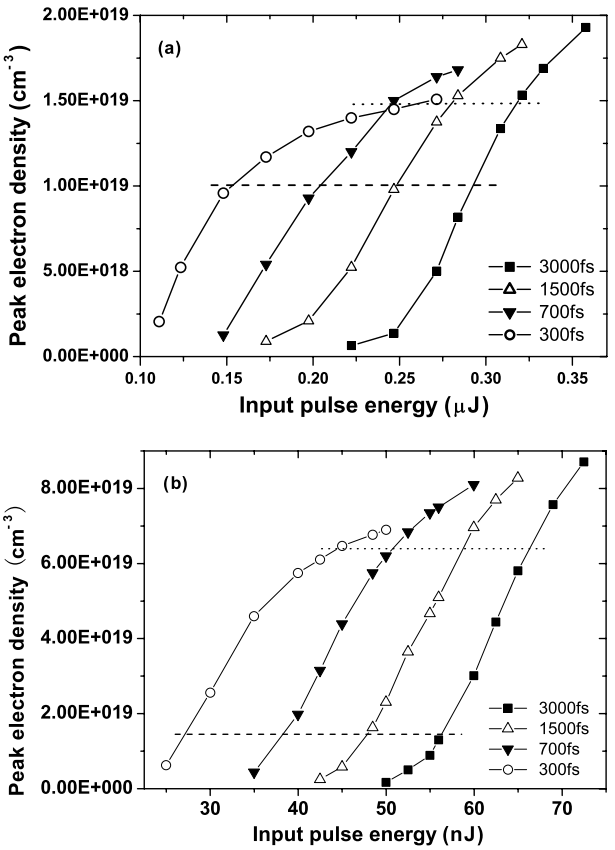

Figure 4. Peak electron densities versus input pulse energy for the two focusing conditions. (a) Effective NA = 0.126, (b) effective NA = 0.255. Squares: $\tau_p = 3000$ fs; up triangles: $\tau_p = 1500$ fs; down triangles: $\tau_p = 700$ fs; circles: $\tau_p = 300$ fs. In (a) the dotted and dashed horizontal lines show the assumed threshold electron density $\rho_{th} = 1.0 \times 10^{19}$ cm^{-3} and 1.45×10^{19} cm^{-3} while in (b) they refer to $\rho_{th} = 1.45 \times 10^{19}$ cm^{-3} and 6.11×10^{19} cm^{-3}.

$\rho_{th} = 6.11 \times 10^{19}$ cm^{-3} it becomes smooth when the pulse duration becomes shorter than 500 fs.

Comparing the experimental results and the theoretical predictions, we can see that in the case of NA = 0.126 a proper criterion of breakdown is $\rho_{th} = 1.45 \times 10^{19}$ cm^{-3}, and for NA = 0.255, $\rho_{th} = 6.11 \times 10^{19}$ cm^{-3} is appropriate. Further analysis show that this difference is a natural result of our experimental definition of LIB. In the experiments the plasma image exhibits a transverse size of about 1.6 μm despite the focusing geometry due to the spatial resolution of the detection system. On the other hand, simulations show that the transverse size of the plasma in both focusing cases, for example FWHM can be defined, are much smaller than 1.6 μm due to the nonlinear mechanism for the generation of the electron. Therefore the luminescence image captured by the detection system is a signal proportional to the integrated electron density over the small breakdown area. Simulations show that for the above different ρ_{th} in the two focusing cases the integrated electron densities are equal to each other within an error range of 6%. That is to say, the fact that the plasma signal observed is proportional to the integrated electron density leads to different electron densities being achieved in the two focusing cases.

Although experimentally we cannot utilize the same electron density as the criterion of breakdown for different focusing geometry, we can easily adopt this definition in our simulation. In figure 3(b) the theoretical thresholds obtained from $\rho_{th} = 1.45 \times 10^{19}$ cm^{-3} for NA = 0.255 are displayed by circles. It can be seen that these thresholds are of course smaller than those from $\rho_{th} = 6.11 \times 10^{19}$ cm^{-3}, but the decreasing tendency of the threshold in this focusing condition remains. That is to say, the different tendencies of the threshold in the two focusing cases is not due to different threshold electron densities being used.

In order to understand the different threshold tendencies, the energy dependence of the peak electron densities (ρ_{peak}) for typical pulse durations is shown in figure 4 for the two focusing conditions. For effective NA = 0.126, the peak electron density exhibits saturation when it exceeds 1.2×10^{19} cm^{-3} for $\tau_p = 300$ fs. In particular, the curves that refer to 300 and 700 fs intersect at $\rho_{peak} = 1.4 \times 10^{19}$ cm^{-3}. Therefore, if ρ_{th} is taken to be larger than 1.4×10^{19} cm^{-3} the breakdown threshold energy for 300 fs will exceed that for 700 fs. In other words, there will be an increase of the thresholds with the decrease of the pulse duration, which is shown in figure 3(a) in the case of $\rho_{th} = 1.45 \times 10^{19}$ cm^{-3}. For the cases where ρ_{th} is assumed to be between 1.4×10^{19} cm^{-3} and 1.0×10^{19} cm^{-3},

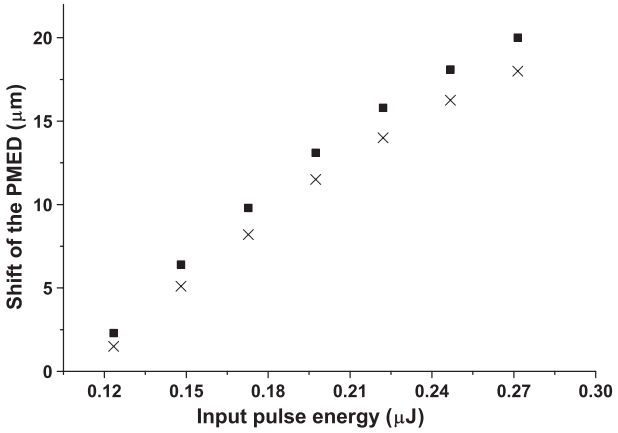

Figure 5. Shifts of the position of the maximum electron density from the geometrical focus versus input pulse energy for $\tau_p = 300$ fs in the case of effective NA = 0.126. Squares: with consideration of self-focusing; crosses: without self-focusing.

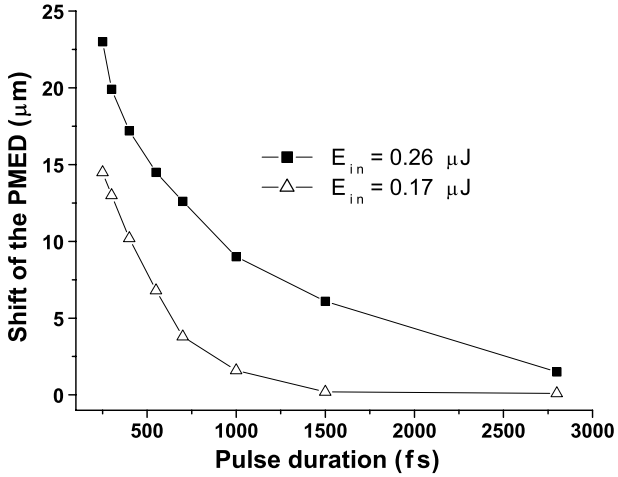

Figure 6. Shifts of the position of the maximum electron density from the geometrical focus for different pulse durations in the case of effective NA = 0.126. Squares: input energy = 0.26 μJ; triangles: input energy = 0.17 μJ.

the breakdown threshold will decrease smoothly, which is also displayed in figure 3(a) for $\rho_{th} = 1.3\times10^{19}$ cm^{-3}. It is obvious that the breakdown threshold energy will drop steadily if ρ_{th} is taken less than 1.0×10^{19} cm^{-3}. In contrast, from figure 4(b) it can be seen that, for effective NA = 0.255, the peak electron density only takes on a slight saturation as it exceeds 5.6×10^{19} cm^{-3} for $\tau_p = 300$ fs. As a result, in figure 3(b) for $\rho_{th} = 6.11 \times 10^{19}$ cm^{-3} the threshold energies tend to smooth when $\tau_p < 600$ fs while for $\rho_{th} = 1.45\times10^{19}$ cm^{-3} a dramatic decrease of the thresholds is predicted.

Based on our calculations we suggest that the defocusing of laser pulse caused by the developing bulk plasma is responsible for the saturation of the electron densities in figure 4(a) and hence the increase of the breakdown thresholds in figure 3(a). Actually, we have noticed that the defocusing effect of the bulk plasma has been suspected to play an important role in the spark formation and material damage of a bulk sample in the femtosecond regime [9]. From equation (2) it is obvious that the electron generation rate is proportional to the laser power density $|\varepsilon|^2$ for avalanche ionization while for MPI it depends on $|\varepsilon|^{2K}$ ($K = 6$). With the decrease of the pulse duration the contribution for electron generation from MPI is expected to become important gradually. As a result, in figures 4(a) and (b) the electron densities of shorter pulse are more likely to saturate than those of longer pulse. At the same time it is known that the defocusing effect can be effectively neglected under tighter external focusing because in this case the plasma is more confined to the focal volume and the pulses propagate through less plasma and experience less defocusing. Therefore we can see that the electron densities in the case of looser focusing are more likely to saturate than those of tighter focusing geometry (see figures 4(a) and (b)). In other words, for relatively shorter pulse and looser focusing the increase of the laser field can be suppressed more effectively by the defocusing, which can lead to the saturation of the peak electron densities when the input pulse energy is high enough in this case.

The role of defocusing can be clearly demonstrated by checking the shift of the position of the maximum electron density (PMED) from the geometrical focus. In fact, defocusing and SF both cause the PMED to move towards the surface of the sample, and so the shift is a joint effect of them. It is well known that SF starts to play a role with increasing peak power; therefore we expect that for pulses of shorter duration the contribution of SF to the shift is more prominent. In figure 5 the shifts versus input energy for $\tau_p = 300$ fs in the case of effective NA = 0.126 is displayed with and without SF[1]. It is found that the shifts without SF are only slightly smaller than those with SF for the same input pulse energy. Therefore we conclude that in our experiments the defocusing effect of the plasma dominate the shift of the PMED and the contribution from SF is insignificant.

The shifts of the PMED versus pulse duration for effective NA = 0.126 are shown in figure 6, where two input energies are used. It can be seen that the shift increases gradually with the decrease of the pulse duration for the same input energy. This fact means that the defocusing becomes more effective for shorter pulse duration, which agrees with our qualitative analysis above. In the case of effective NA = 0.225, it is found that the shifts of PMED are smaller than 3 μm for all input pulse energies used in our simulation, which demonstrates that the effect of defocusing is insignificant in this focusing condition in our study. These results support the defocusing of plasma being responsible for the increase of LIB threshold with decrease of pulse duration for effective NA = 0.126.

4. Conclusion

We have measured the laser-induced breakdown thresholds in bulk fused silica as a function of the laser pulse duration. It was found that the breakdown thresholds exhibited different tendencies in the subpicosecond regime for different focusing conditions. Our simulations reproduced the experimental observation and we found that the defocusing effect of developing bulk plasma played a crucial role for relatively looser external focusing and was responsible for the increase of the threshold energy observed in our experiments. It was also noticeable that the predicted tendency of the threshold

[1] In the calculation the effect of self-focusing can easily be omitted by setting $n_2 = 0$.

energy on pulse duration was sensitive to the threshold plasma density used as the onset of the breakdown, which implied that different diagnostic methods may provide different threshold tendencies.

Acknowledgments

This work was supported by the National Key Basic Research Special Foundation (NKBRSF) under Grant No. TG1999075207, and the National Science Foundation of China under Grant Nos 10104003 and 90101027. The project was also sponsored by Youth Teacher's Foundations of National Education Ministry and the Scientific Research Foundation for Returned Overseas Chinese Scholars of National Education Ministry.

References

[1] Bloembergen N 1974 *IEEE J. Quantum Electron.* **10** 375
[2] Du D, Liu X, Korn G, Squire J and Mourou G 1994 *Appl. Phys. Lett.* **64** 3071
[3] Du D, Liu X and Mourou G 1996 *Appl. Phys.* B **63** 617
[4] Stuart B C, Feit M D, Rubenchik A M, Shore B W and Perry M D 1995 *Phys. Rev. Lett.* **74** 2248
[5] Stuart B C, Feit M D, Rubenchik A M, Shore B W and Perry M D 1996 *J. Opt. Soc. Am.* B **13** 459
[6] Varel H, Ashkenasi D, Rosenfeld A, Herrmann R, Noack F and Campbell E E B 1996 *Appl. Phys.* A **62** 293
[7] Lenzner M, Krüger J, Sartania S, Cheng Z, Spielmann Ch, Mourou G, Kautek W and Krausz F 1998 *Phys. Rev. Lett.* **80** 4076
[8] Tien A C, Backus S, Kapteyn H, Murnane M and Mourou G 1999 *Phys. Rev. Lett.* **82** 3883
[9] von der Linde D and Schüler H 1996 *J. Opt. Soc. Am.* B **13** 216
[10] Perry M D and Mourou G 1994 *Science* **264** 917
[11] Amoruso S, Bruzzaese R, Spinell N and Velotta R 1999 *J. Phys. B: At. Mol. Opt. Phys.* **32** 131
[12] Chen L M, Zhang J, Teng H, Dong Q L, Chen Z L, Liang T J, Zhao L Z and Wei Z Y 2001 *Phys. Rev.* E **63** 036403
[13] Schaffer C B, Brodeur A and Mazur E 2001 *Meas. Sci. Technol.* **12** 1784
[14] Nguyen N T, Saliminia A, Liu W, Chin S L and Vallée R 2003 *Opt. Lett.* **28** 1591
[15] Wu Z X, Jiang H B, Yang H and Gong Q H 2003 *J. Opt. A: Pure Appl. Opt.* **5** 102
[16] Wu Z X, Jiang H B, Luo L, Guo H C, Yang H and Gong Q H 2002 *Opt. Lett.* **27** 448
[17] Sudrie L, Couairon A, Franco M, Lamouroux B, Prade B, Tzorztakis S and Mysyrowicz A 2002 *Phys. Rev. Lett.* **89** 186601
[18] Ward H and Bergé L 2003 *Phys. Rev. Lett.* **90** 053901
[19] Feng Q, Moloney J V, Newell A C, Wright E M, Cook K, Kenney P K, Hammer D X, Rockwell B A and Thompson C R 1997 *IEEE J. Quantum Electron.* **33** 127
[20] Feit M D and Fleck J A Jr 1974 *Appl. Phys. Lett.* **24** 169
[21] Sun Q, Jiang H B, Liu Y, Yang H and Gong Q H 2005 *Opt. Lett.* **30** 320
[22] Guo H C, Jiang H B, Fang Y, Peng C, Yang H, Li Y and Gong Q H 2004 *J. Opt. A: Pure Appl. Opt.* **6** 787

View publication stats